through paraconodonts, to euconodonts or "true" conodonts (*19*) such as the Waukesha animal. In addition, there is no structure in chaetognaths equivalent to the segmentation in the fossil. The euconodonts, at least, may be more closely related to the chordates.

In addition to the exceptional preservation of soft-bodied taxa, an important aspect of this biota is the absence or rarity of most shelly groups normally found in Silurian assemblages. Echinoderms, mollusks, brachiopods, bryozoans, and corals are all very rare. Only trilobites are abundant and diverse. These factors suggest that the Waukesha biota represents unusual environmental conditions as well as taphonomic processes. The only comparable *Lagerstätten* from the Silurian occur in the inliers of southern Scotland (*20*), but these are dominated by fish and eurypterids.

DONALD G. MIKULIC
Illinois State Geological Survey, Champaign 61820
DEREK E. G. BRIGGS
Department of Earth Sciences, Goldsmiths' College, University of London, London SE8 3BU, England
JOANNE KLUESSENDORF
Department of Geology, University of Illinois, Urbana 61801

References and Notes

1. Konservat-Lagerstätten are sediment bodies that yield an unusual amount of paleontological information because of incomplete decay of protein in the organic remains. A. Seilacher, *Neues Jahrb. Geol. Palaeontol. Monatsh.* **1970** (H.1), 34 (1970).
2. D. H. Collins, D. E. G. Briggs, S. Conway Morris, *Science* **222**, 163 (1983); H. B. Whittington, *Proc. Geol. Assoc. London* **91**, 127 (1980); S. Conway Morris and H. B. Whittington, *Sci. Am.* **241**, 122 (July 1979).
3. W. Stürmer and J. Bergström, *Palaeontol. Z.* **47**, 104 (1973); *ibid.* **50**, 78 (1976); *ibid.* **52**, 57 (1978).
4. This is informal usage pending revision.
5. W. B. N. Berry and J. Barrick, personal communications.
6. R. Norby, personal communication.
7. I. Chlupáč, *Palaeontology* **6**, 97 (1963); D. E. G. Briggs and W. D. I. Rolfe, *Spec. Pap. Palaeontol.* **30**, 249 (1983).
8. G. Pinna, P. Arduini, C. Pesarini, G. Terruzzi, *Atti. Soc. Ital. Sci. Nat. Mus. Civ. Stor. Nat. Milano* **123**, 469 (1982); S. Secretan and B. Riou, *Ann. Paleontol. Invertebr.* **69**, 59 (1983).
9. W. Stürmer and J. Bergström, *Palaeontol. Z.* **55**, 237 (1981).
10. N. Eldredge, *Am. Mus. Novit. No. 2543* (1974).
11. H. B. Whittington, *Philos. Trans. R. Soc. London Ser. B* **284**, 165 (1978); R. A. Robison, *J. Paleontol.*, in press.
12. J. E. Almond, *Philos. Trans. R. Soc. London Ser. B*, in press; W. D. I. Rolfe, in *The Terrestrial Environment and the Origin of Land Vertebrates*, A. L. Panchen, Ed. (Systematics Association, London, 1980), pp. 117–157.
13. P. Tasch, in *Treatise on Invertebrate Paleontology*, part R, *Arthropoda 4*, R. C. Moore, Ed. (Geological Society of America and University of Kansas Press, Lawrence, 1969), vol. 1, pp. 128–191.
14. Compound eyes and biramous appendages, for example, do not occur in nymphs [W. D. I. Rolfe, *Palaeontology* **10**, 307 (1967)].
15. J. Yager, *J. Crust. Biol.* **1**, 328 (1981); H. K. Brooks, *J. Paleontol.* **29**, 852 (1955).
16. S. Conway Morris, R. K. Pickerill, T. L. Harland, *Can. J. Earth Sci.* **19**, 2150 (1982); S. Conway Morris, *Spec. Pap. Palaeontol.* **20**, 1 (1977).
17. H. Kozur, *Lethaia* **3**, 225 (1970); S. Conway Morris, *Parasitology* **82**, 489 (1981).
18. D. E. G. Briggs *et al.*, *Lethaia* **16**, 1 (1983).
19. H. Szaniawski, *J. Paleontol.* **56**, 806 (1982); S. Bengtson, *Lethaia* **9**, 185 (1976); *Fossils Strata* **15**, 5 (1983).
20. W. D. I. Rolfe, in *Excursion Guide to the Geology of the Glasgow District*, B. J. Bluck, Ed. (Geological Society of Glasgow, Glasgow, Scotland, 1973), pp. 119–126.
21. We thank E. Reeseman, D. Dewey, R. Hodgins, D. Green, and W. Knuese of Waukesha Lime & Stone Company for permission and aid in collecting and for donating material, much of which was collected by G. Gunderson and R. Meyer, who also discovered some of the taxa; K. Westphal and the Department of Geology at the University of Wisconsin for loan of specimens; C. Klug, S. LoDuca, and S. Mikulic for field assistance; and D. B. Blake and the Field Museum of Natural History for facilities. P. Graham carried out x-ray diffraction analysis. D. B. Blake, S. Conway Morris, and R. L. Langenheim, Jr., reviewed the report. R. J. Aldridge and M. P. Smith discussed the conodont animal. D.E.G.B. was supported by Goldsmiths' College Research Fund, the Royal Society, and the Field Museum Visiting Scientist Program. J.K. was supported in part by a grant-in-aid from Sigma Xi, the Scientific Research Society, and the Department of Geology and Graduate College, University of Illinois.

11 December 1984; accepted 14 January 1985

Study by Synchrotron Radiation of the Structure of a Working Catalyst at High Temperatures and Pressures

Abstract. *A relation among activity, composition, and structure was determined for a working catalyst by means of a stainless-steel reactor cell of novel design that permitted operation at temperatures and pressures similar to those in industrial reactors. Molybdenum K-edge x-ray absorption spectra were used to probe the structural environment of molybdenum in CoMoS/γ-alumina catalysts while hydrodesulfurization of benzothiophene was proceeding at high temperature and pressure. For catalyst samples with different contents of cobalt, radial structure functions obtained from extended x-ray absorption fine structure data presented the same features as those obtained from the spectra of MoS_2/γ-alumina reference samples. Moreover, Mo–S and Mo–Mo coordination numbers were maximum for the sample with an atomic ratio of Co to (Co + Mo) of 0.33; this sample was also the most active catalyst tested.*

Heterogeneous catalysts are used in the majority of industrial chemical processes, most of which take place at pressures and temperatures far removed from ambient conditions. Catalytic materials are examined by various physical techniques (*1, 2*), including most recently x-ray absorption spectroscopy (*3–5*). In particular, extended x-ray absorption fine structure (EXAFS) has become a useful technique for determining structural parameters (such as interatomic distances and coordination numbers) of supported metal catalysts where the metal is in the form of clusters less than 1 nm in size (*6*). However, most previous studies have been done with the catalyst sample in a nonreactive atmosphere under ambient conditions of pressure and temperature, before and after the chemical reaction took place. The assumption that the catalyst does not change during cooling and depressurization was implicit in the analysis of those results.

The study of a catalyst under realistic reaction conditions in situ has been a long-sought goal in heterogeneous catalysis (*7*). Earlier we observed that the structure of a hydrodesulfurization (HDS) catalyst did not change during reaction (*8*). We now describe catalysts of different composition and measure their rates of reaction.

In view of increasing concerns about the environmental impact of sulfur, perhaps one of the most important catalytic processes in refining oil and synthetic fuels is the HDS of hydrocarbons. The removal of sulfur from oil fractions or coal slurries is accomplished by the reaction of sulfur-containing species with hydrogen gas on molybdenum- or tungsten-based catalysts promoted by cobalt or nickel atoms (*9*). In HDS, the sulfur is removed as H_2S gas. Hydrotreating crude oil is a major process in refining. Removal of sulfur from crude oil is necessary not only because of SO_2 emission restrictions but also because of catalyst poisoning by sulfur compounds in other refinery processes. Because of the continuing depletion of petroleum resources, larger quantities of lower grade, high-sulfur crude oils are reaching the refineries, and the trend is likely to continue. Efforts have been directed toward describing the structure of HDS catalysts so that the relation between structure and HDS activity can be understood.

We have designed a reactor cell in which the absorption of x-rays by HDS catalysts can be measured while the reaction is carried out under pressures and temperatures similar to those in industry (*10*). The x-rays enter the cell through a thin beryllium window and pass through the catalyst before leaving the cell through a second beryllium window. The intensity of the x-ray beam is measured

Table 1. Structure parameters and site-time yield for hydrodesulfurization of benzothiophene. Total pressure was 7.3 MPa and 1 atm for spectra taken at 523 K and at room temperature, respectively. Flow rates throughout the experiment were 5 liters per hour (standard temperature and pressure) and 6 ml per hour for gas and liquid feeds, respectively. Total benzothiophene conversions varied between 60 and 70 percent. R.T., room temperature.

Ratio*	Temperature (Kelvin)	Coordination number†		Bond length (picometers)		ν_t‡ (second^{-1})
		Mo–S	Mo–Mo	Mo–S	Mo–Mo	
0.0	523	4.5	1.6	240	316	0.06
0.13	523	4.7		239		0.26
	R.T.	4.8	2.9	240	315	
0.33	523	6.3	4.4	240	314	0.40
	R.T.	6.0	3.8	240	314	
0.72	523	5.1	2.2	240	315	0.27

*Ratio of Co to (Co + Mo). †For the first coordination shell. ‡Nominal site-time yield (the number of molecules of ethylbenzene produced per molybdenum atom in the catalyst per second).

just outside the inlet and outlet windows so that the absorption coefficient of the catalyst can be calculated. The powder catalyst is compacted in the form of a thin wafer and held in the path of the beam by a sample holder, which also contains gas and liquid inlets. In this way, the fresh reactants flow in a film down the surface of the catalyst, which approximates the conditions in industrial trickle-bed reactors. The extent of reaction can be measured by analyzing the inlet and outlet flows.

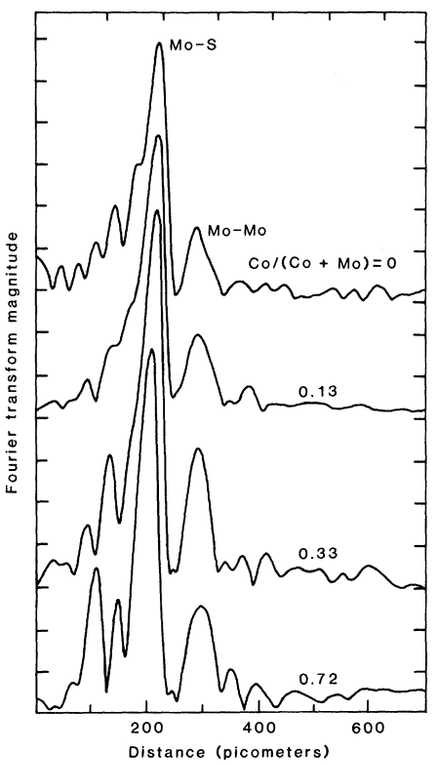

Fig. 1. Radial structure function around a molybdenum atom for CoMoS/γ-Al_2O_3 samples with different atomic ratios of Co to (Co + Mo) during reaction at 523 K and 7.3 MPa. The reactor was fed with hydrogen (99.95 percent; Liquid Carbonic) and a 7 weight-percent solution of benzothiophene (97 percent; Aldrich) in Decalin (97 percent; Fisher).

The x-ray absorption coefficient of an absorbing atom presents modulations in the high-energy side of an absorption edge. These EXAFS modulations are generated when the electron ejected by x-ray absorption interferes constructively or destructively with the electrons of the surrounding atoms. Three types of information are generally obtained from the analysis of the EXAFS modulations: R, the interatomic distance; N, the coordination number; and σ, the correlated Debye-Waller factor. The strengths and limitations of EXAFS as a technique for structural characterization have been reviewed (*11*).

The molybdenum K-edge EXAFS of CoMoS/γ-Al_2O_3 catalysts has been measured under ambient conditions by several investigators. The features in these spectra closely resembled those in the spectrum of MoS_2 (*3–5*). Thus, we used as references the spectra of MoS_2 mixed with alumina taken at room temperature and under reaction conditions. The radial structure function (RSF) for this model compound has been described (*5*). Two peaks occur at 198 and 284 pm, representing the six sulfur and six molybdenum neighbors that make the first Mo–S and Mo–Mo shells, respectively. These distances correspond to a phase shift of 43 and 32 pm from the actual Mo–S (241 pm) and Mo–Mo (316 pm) distances, respectively. Scattering from the second Mo–S and second and third Mo–Mo shells also occurs. The amplitudes of all peaks decrease with increasing temperature because of thermal vibrations (*8*).

Amplitude and phase-shift functions of the catalyst and model compound were calculated. A nonlinear least-squares fitting routine was used to adjust the functions of the catalyst to those corresponding to the model compound by varying R, N, and σ (Table 1). The catalyst used has been described (*3*). Approximately 1-g portions of the catalyst powders were subjected to pressures of 10 MPa, resulting in wafers 1.3 mm thick and 2.54 cm in diameter. The RSF's obtained from EXAFS spectra taken during the HDS of benzothiophene at 523 K and 7.3 MPa (Fig. 1) showed two major peaks in all four CoMoS/γ-Al_2O_3 samples. The first peak at about 190 pm represents a Mo–S bond of 241 pm. A second peak at about 290 pm corresponds to the first Mo–Mo shell (actual bond length, 316 pm). Both the Mo–S distance and the Mo–Mo distance on these catalysts under reaction are in agreement with the interatomic distances for crystalline MoS_2. However, the main peaks in Fig. 1 are smaller than the corresponding peaks on the model compound, indicating a lower coordination number in the catalysts.

There were no major differences between the RSF's obtained from spectra taken at room temperature immediately after reaction (Fig. 2) and those in Fig. 1; both sets present peaks for the first Mo–S and Mo–Mo coordination shells with bond lengths corresponding to those observed for MoS_2. This seems to indicate that the structure of the molybdenum environment may not be affected by depressurization and cooling.

The final products of the HDS of benzothiophene are ethylbenzene and H_2S.

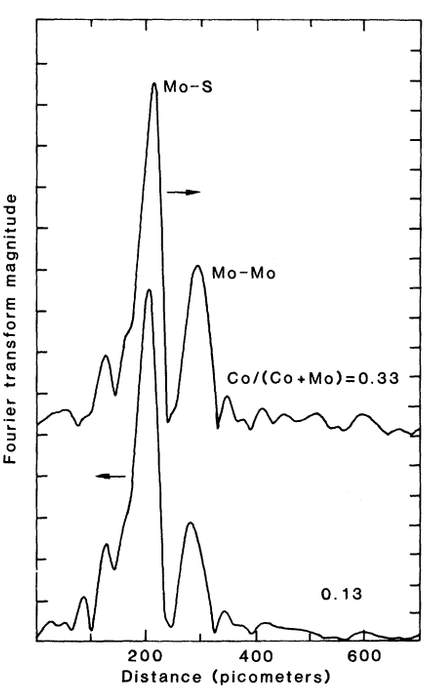

Fig. 2. Radial structure function around a molybdenum atom for CoMoS/γ-Al_2O_3 samples at room temperature after reaction. The gas phase was hydrogen (99.95 percent; Liquid Carbonic) at atmospheric pressure.

As shown in Table 1, the rate of production of ethylbenzene was maximum for the catalyst with the largest Mo–Mo and Mo–S coordination numbers. This is in agreement with results obtained earlier in this laboratory (*3*) that showed a similar relationship between the rate of HDS of thiophene and Mo–S coordination number determined in a less precise way.

We have observed a double correlation under real conditions of operation and with a working catalyst between HDS activity on the one hand and catalyst composition and structure on the other hand. Further work is under way to determine the nature of this correlation.

M. BOUDART
R. A. DALLA BETTA
K. FOGER
D. G. LÖFFLER
M. G. SAMANT
Department of Chemical Engineering, Stanford University, Stanford, California 94305

References and Notes

1. B. G. Silbernagel, T. A. Pecoraro, R. R. Chianelli, *J. Catal.* **78**, 380 (1982).
2. F. E. Massoth *et al.*, *ibid.* **85**, 53 (1984).
3. M. Boudart, J. Sánchez Arrieta, R. A. Dalla Betta, *J. Am. Chem. Soc.* **105**, 295 (1984).
4. B. S. Clausen, H. Topsøe, R. Candia, B. Lengeler, *ACS Symp. Ser.* **24**, 71 (1984).
5. T. G. Perham and R. P. Merrill, *J. Catal.* **85**, 295 (1984).
6. J. H. Sinfelt, *Bimetallic Catalysts: Discoveries, Concepts, and Applications* (Wiley, New York, 1983), pp. 63–82 and 98–111.
7. K. Tamaru, *Dynamic Heterogeneous Catalysis* (Academic Press, London, 1978), pp. vii and viii.
8. M. Boudart, R. Dalla Betta, K. Foger, D. G. Löffler, *Springer Proc. Phys.* **2**, 187 (1984).
9. B. C. Gates, J. R. Katzer, G. C. A. Schuit, *Chemistry of Catalytic Processes* (McGraw-Hill, New York, 1979), pp. 390–422.
10. R. A. Dalla Betta, M. Boudart, K. Foger, D. G. Löffler, J. Sánchez Arrieta, *Rev. Sci. Instr.* **55**, 1910 (1984).
11. P. A. Lee, P. H. Citrin, P. Eisenberger, B. M. Kincaid, *Rev. Mod. Phys. Part I* **53**, 769 (1981).
12. Supported by grant DE-FG22-83PC60782 from the U.S. Department of Energy (Fossil Energy Division) and carried out in part at the Stanford Synchrotron Radiation Laboratory (supported by the U.S. Department of Energy). K.F., on leave from the Commonwealth Scientific and Industrial Research Organization, Division of Materials Science (Australia), and D.G.L., on leave from the Universidad Nacional de Mar del Plata and Consejo Nacional de Investigaciones Científicas y Técnicas (Argentina), acknowledge support from their home organizations.

17 December 1984; accepted 13 February 1985

Coupling of *Tetrahymena* Ribosomal RNA Splicing to β-Galactosidase Expression in *Escherichia coli*

Abstract. *Splicing of the* Tetrahymena *ribosomal RNA precursor is mediated by the folded structure of the RNA molecule and therefore occurs in the absence of any protein in vitro. The* Tetrahymena *intervening sequence (IVS) has been inserted into the gene for the α-donor fragment of β-galactosidase in a recombinant plasmid. Production of functional β-galactosidase is dependent on RNA splicing in vivo in* Escherichia coli. *Thus RNA self-splicing can occur at a rate sufficient to support gene expression in a prokaryote, despite the likely presence of ribosomes on the nascent RNA. The β-galactosidase messenger RNA splicing system provides a useful method for screening for splicing-defective mutations, several of which have been characterized.*

Many eukaryotic genes contain introns, or intervening sequences (IVS), that must be removed from their RNA transcripts by a cleavage-ligation reaction termed RNA splicing (*1*). In one class of splicing reactions the RNA mediates its own splicing. Examples include the nuclear ribosomal RNA (rRNA) precursor of the ciliated protozoan *Tetrahymena* (*2, 3*), as well as various mitochondrial messenger RNA (mRNA) and rRNA precursors in fungi (*4*). The RNA lowers the activation energy for specific cleavage-ligation reactions by providing a binding site for guanosine, one of the reactants, and by straining or activating the phosphates at the splice sites (*5, 6*). In addition, a portion of the IVS may bind one or both adjacent rRNA coding regions (exons) to facilitate their ligation (*7*).

RNA self-splicing in vitro requires only monovalent and divalent cations and some form of the nucleoside guanosine (*2, 3*). We therefore reasoned that it should take place to some extent in vivo, even in a prokaryotic cell where RNA splicing is not a normal feature of gene expression. We have now tested this idea by inserting the *Tetrahymena* IVS and a small portion of the exons within sequences coding for β-galactosidase. Both genetic and physical evidence support the conclusion that accurate RNA splicing occurs in *E. coli* to produce functional mRNA. The system has been used to isolate mutants that are defective in splicing. Thus, classical genetic techniques can now be used to investigate structure-function relations in the self-splicing IVS.

Plasmid pUC8 encodes the NH_2-terminal portion (α-donor fragment) of the β-galactosidase protein (*8*). The α-donor polypeptide can combine with a defective β-galactosidase protein (α-acceptor) to restore enzyme activity (*9*). A fragment of the *Tetrahymena* rRNA gene containing the IVS was inserted in the Bam HI restriction site within the α-donor coding region of pUC8 (Fig. 1A). The 413-nucleotide IVS contains stop codons in all three reading frames, which would cause premature termination of α-donor translation. If RNA splicing occurred, however, the small portions of the exons included in the insert would be joined to give an open reading frame. Extra amino acids can be tolerated in the α-donor fragment without destroying activity. Thus, β-galactosidase expression would be contingent on RNA splicing (Fig. 1B).

Escherichia coli strain JM83 (*8*) was transformed with the recombinant plasmids and plated on agar containing ampicillin and X-gal (5-bromo-4-chloro-3-indolyl-β-D-galactoside). X-gal is a histochemical substrate for β-galactosidase and is converted to a blue dye after hydrolysis by the enzyme. Approximately half of the colonies were white (no β-galactosidase expression); the remainder were mostly very pale blue, while a few were blue. Restriction endonuclease cleavage analysis of plasmids from three colonies of each color group indicated that the white colonies contained the *Tetrahymena* insert in the incorrect orientation, whereas the blue and very pale blue colonies contained the insert in the correct orientation. Nucleotide sequencing of plasmids from three blue colonies (including pβG-IVS1) indicated that in each case one nucleotide had been inserted at the upstream Bam HI site during cloning (Fig. 1C). The deletion was such that the open reading frame of the ligated exons was put in-frame with the β-galactosidase coding sequences. Translation of the resulting mRNA would give an α-donor polypeptide containing 18 amino acids more than that produced by pUC8, and should give β-galactosidase activity (*10*). In the plasmids from the very pale blue colonies, such as pβG-IVS13, both Bam HI sites were intact (Fig. 1C). Sequencing indicated two termination codons in the protein reading frame, which should eliminate β-galactosidase activity (*8*). The residual β-galactosidase activity conferred by these plasmids may be due to occasional splicing to a site upstream from the termination codons in the correct reading frame.

Several lines of evidence indicate that production of β-galactosidase in pβG-IVS1 is dependent on proper splicing of the α-donor pre-mRNA. The extra nu-